Available online at www.sciencedirect.com

Journal of Photochemistry and Photobiology A: Chemistry 171 (2005) 21–26

Journal of Photochemistry and Photobiology A:Chemistry

www.elsevier.com/locate/jphotochem

N_2 laser-induced formation of copolymeric ultrafine particles in a gaseous tetraethenylgermane–carbon disulfide mixture

Hiroshi Morita[a,b,*], Katsuhiko Semba[a], Zdeněk Bastl[c], Jan Šubrt[d], Josef Pola[e]

[a] Graduate School of Science and Technology, Chiba University, Yayoi-cho, Inage-ku, Chiba 263-8522, Japan
[b] Department of Information and Image Sciences, Faculty of Engineering, Chiba University, Yayoi-cho, Inage-ku, Chiba 263-8522, Japan
[c] J. Heyrovský Institute of Physical Chemistry, Academy of Sciences of the Czech Republic, 18223 Prague, Czech Republic
[d] Institute of Inorganic Chemistry, Academy of Sciences of the Czech Republic, 25086 Řež near Prague, Czech Republic
[e] Institute of Chemical Process Fundamentals, Academy of Sciences of the Czech Republic, 16502 Prague, Czech Republic

Received 31 May 2004; received in revised form 26 July 2004; accepted 24 August 2004

Abstract

N_2 laser light irradiation upon a gaseous mixture of carbon disulfide (CS_2) and tetraethenylgermane (TEG) induced unique co-polymerization of both molecules, which resulted in the formation of composite TEG/CS_2 sedimentary aerosol particles. The chemical structure of the particles assessed by EDX–SEM, XP and FT-IR spectral analyses was compatible with the incorporation of TEG into photo-polymerizing CS_2 through reaction at the ethenyl group.

Keywords: Ultrafine particles; Photo-polymerization; Tetraethenylgermane; Carbon disulfide

1. Introduction

Laser-induced polymerization in the gas phase attracts interest due to its suitability for chemical vapor deposition of novel materials [1–8] and for synthesis of ultrafine and nano-particles to develop novel optoelectronic devices [9,10]. The laser-induced gas phase polymerization of organic and organosilicon compounds has been achieved via (a) polymerization of short-lived species (e.g. silenes [11], silanones [8,12], methanimine [13], pyridinyl radicals [2]) generated in high concentrations through photo-decomposition of gaseous precursors, or via (b) UV laser excitation of methyl acrylate [14], acrolein [15,16] and carbon disulfide (CS_2) [17–22].

CS_2 is a reactive molecule suitable to produce composite aerosol particles with acrolein [23] and methyl acrylate [24,25] under UV light irradiation. Chemical structure of the aerosol particles produced photochemically from pure CS_2 was described as $(CS_2)_x$ polymer [26,27], a blend of C polymer and S polymer [28], $(CS)_x$ polymer [17,18,22], or a mixture of $(CS_2)_x$ and $(C_3S_2)_x$ [29]. These different views having been based on vibrational spectral data and/or theoretical treatments compete in the structure assignment.

Alkyl(alkoxy)germanes have attracted interest in producing solid materials by using chemical vapor deposition (CVD) of IR laser [30,31]. Compared to organosilicon compounds, organogermanium compounds have less tendency towards polymerization and bond breakage is easier in Ge–C bond than in Si–C bond [32]. Due to these facts, IR laser-driven CVD of tetramethylgermane produced brown material, which is rich in Ge atom [33].

In the present paper, in order to involve organogermanium compounds in ultrafine particles we have undertaken to synthesize aerosol particles from a gaseous mixture of CS_2 and tetraethenylgermane (TEG) under N_2 laser light irradiation. Special attention has been paid to two-photon absorption of N_2 laser light [34] to investigate whether TEG molecules can initiate polymerization reaction in the gaseous mixture.

---

* Corresponding author. Tel.: +81 43 290 3471; fax: +81 43 290 3490.
E-mail address: hmorita@faculty.chiba-u.jp (H. Morita).

1010-6030/$ – see front matter © 2004 Elsevier B.V. All rights reserved.
doi:10.1016/j.jphotochem.2004.08.019

N_2 laser light irradiation on the CS_2–TEG gaseous mixture resulted in the production of sedimentary aerosol particles. Chemical structures of the sedimentary particles were elucidated by means of FT-IR and X-ray photoelectron spectroscopy (XPS) and by EDX–SEM technique, and the nucleation process in aerosol particle formation was investigated by measuring monitor (He–Ne laser) light intensity scattered by the formed aerosol particles.

2. Experimental

CS_2 (Kanto, >99%, G.R. grade) and TEG (>96%, prepared using the method by Seyferth [35]) were degassed by several (at least three) freeze–pump–thaw cycles and purified by vacuum distillation prior to use. Each gaseous sample was admitted into a cross-shaped Pyrex cell having a long (length 155 mm, inner diameter, i.d. 35 mm) and short (length 80 mm, i.d. 20 mm) arms equipped with a couple of quartz and KBr windows through a vacuum line equipped with a capacitance manometer (Edwards Barocel Type 600). The background pressure of the irradiation cell was less than 8×10^{-5} Torr (1 Torr = 133.3 Pa). Gaseous samples were irradiated with N_2 laser light (Lumonics HE-440, 337.1 nm, pulse width 10 ns) at an energy of 1.8 mJ/pulse effective on the area of 3 cm^2 at a repetition rate of 12 Hz. Laser power was measured with a pyroelectric joulemeter (Gentec ED-500) combined with a synchroscope (Iwatsu SS-7810). Monitor (He–Ne laser) light intensity scattered by the aerosol particles floating in the cell was measured with a combination of a photomultiplier tube (EMI 6256S) and a lock-in amplifier (SRS SR-530) by chopping and synchronizing the monitor light with exciting N_2 laser pulses by using a delay and pulse generator (SRS DG535). FT-IR spectra of a gaseous mixture of CS_2 and TEG and of pure gaseous TEG in the irradiation cell before and after the N_2 laser irradiation were measured with a Nicolet NEXAS 670 FT-IR spectrometer. The depletion of TEG and CS_2 was followed using diagnostic bands at 3060 and 1005 cm^{-1} for TEG and 1532 cm^{-1} for CS_2. Formation of ethyne was monitored at 730 cm^{-1}. The aerosol particles were deposited on a Cu sheet accommodated in the irradiation cell. In order to measure their chemical and physical properties, these samples had to be transported from the irradiation cell and exposed to ambient atmosphere. Scanning electron microscopy (SEM) images of sedimentary aerosol particles were taken with a Topcon ABT-32 and a Philips XL30 CP scanning electron microscope. X-ray photoelectron spectra (XPS) were measured with a Gammadata Scienta ESCA 310 electron spectrometer using monochromatized Al Kα ($h\nu$ = 1486.6 eV) radiation for electron excitation. The spectra of Ge $2p_{3/2}$, C 1s, O 1s and S 2p photoelectrons were measured. Curve fitting of high-resolution spectra was accomplished using the lines of Gaussian–Lorentzian shape, and binding energies were estimated within an error limit of ±0.2 eV. Photoelectron peak areas were calculated after removal of Shirley background. The quantification of the superficial elemental concentrations was carried out by correcting the peak areas for the pertinent photo-ionization cross-sections and electron analyser transmission function and by accounting for the dependence of the electron inelastic mean free paths on the kinetic energy.

3. Results and discussion

3.1. Laser photolysis

N_2 laser irradiation on a gaseous mixture of CS_2 (20 Torr) and TEG (5 Torr) for 2 h resulted in the formation of sedimentary aerosol particles of yellowish-white color, which deposited on a Cu substrate accommodated at the bottom of the irradiation cell (yield: 0.1 mg) with a reproducible sedimentation pattern. On the other hand, pure TEG vapor (5 Torr) did not produce any deposited material under prolonged irradiation for 7 h of N_2 laser light.

The nucleation process in aerosol particle formation was monitored by measuring the He–Ne laser light intensity scattered by aerosol particles, which were formed under N_2 laser light irradiation. The results are shown in Fig. 1. With increasing partial pressure of CS_2 from 10 to 20 Torr at a fixed partial pressure of TEG (5 Torr), the scattered light intensity

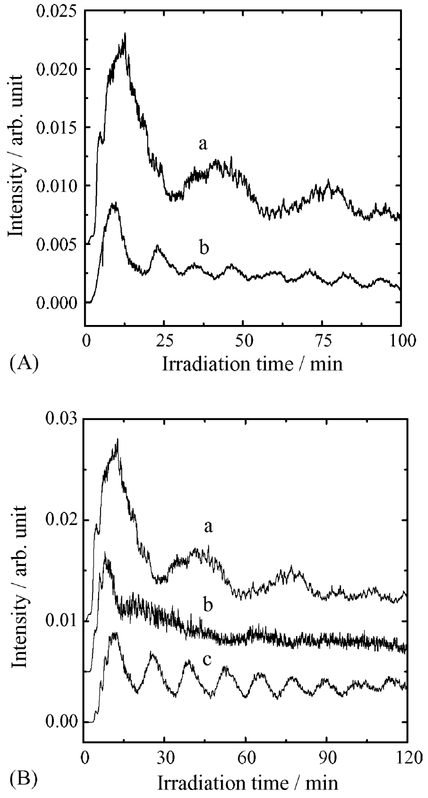

Fig. 1. He–Ne laser light intensity scattered by the aerosol particles produced from a gaseous mixture of CS_2 and TEG under N_2 laser irradiation at an energy of 1.8 mJ/pulse. Respective partial pressures (in Torr) of CS_2 and TEG were (a) 20 and 5, (b) 10 and 5 (A); (a) 20 and 5, (b) 20 and 3, (c) 20 and 0 (B).The ordinates are shifted consequtively by 0.005.

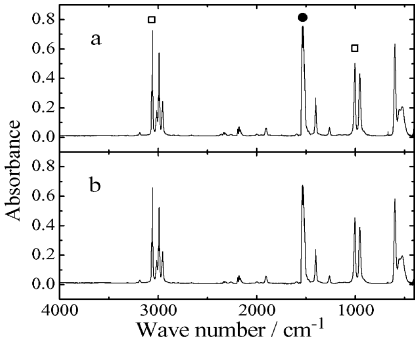

Fig. 2. FT-IR spectra of a gaseous mixture of CS_2 (10 Torr) and TEG (5 Torr) (a) before light irradiation and (b) after 7 h irradiation of N_2 laser light. Depletion rates were evaluated at 1532 cm^{-1} band of CS_2 (●) and at 3060 and 1005 cm^{-1} bands of TEG(□).

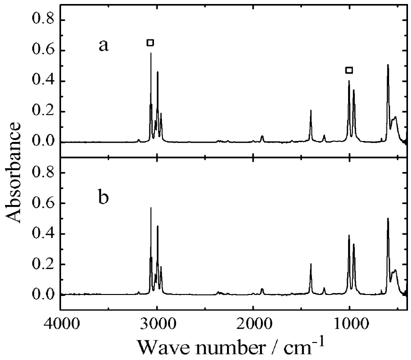

Fig. 3. FT-IR spectra of pure TEG (5 Torr) (a) before light irradiation and (b) after 7 h irradiation of N_2 laser light. Depletion rate was evaluated at 3060 and 1005 cm^{-1} bands of TEG(□).

increased and the induction period to detect scattered light became shorter (from 110 to 50 s) (Fig. 1A). During the induction period to detect scattered light, nucleation reaction proceeds followed by particle growth. Hence, the induction period is a measure of relative rate of nucleation and propagation reactions in aerosol particle formation. Scattered light intensity after reaching its maximum value is proportional to the number of aerosol particles with various particle sizes in cases where the particle size distribution is not dependent on irradiation time of exciting light as in the present experimental conditions [34]. The increase in the scattered light intensity and the shortening of the induction period (from 210 to 130 s and further to 50 s at 0, 3 and 5 Torr of TEG, respectively) were also observed with increasing partial pressure of TEG (Fig. 1B). These results clearly showed that both CS_2 and TEG molecules contributed to the nucleation process by which the aerosol particles are formed. Note that fluctuations of the scattered light intensity with long and short periods were frequently observed in the nucleation processes involving CS_2 molecules. These fluctuations are believed to be due to the temporal and local pressure change of reactant gaseous molecules caused by the formation and sedimentation of the aerosol particles and to be due to the convection of entire gaseous sample [17–19].

The N_2 laser-induced chemical processes were investigated for a gaseous mixture of CS_2 (10 Torr) and TEG (5 Torr) and for pure TEG (5 Torr) through FT-IR spectra (Figs. 2 and 3). The spectrum of the mixture before the light irradiation coincided with the superimposed spectra of the individual CS_2 and TEG, showing the absence of chemical reaction and complex formation between the components. After the light irradiation, FT-IR spectra of the gaseous samples were measured after allowing for complete sedimentation of the formed aerosol particles. All the band intensities of the gaseous molecules decreased and very weak ethyne band appeared at 730 cm^{-1}. In a typical 7 h irradiation experiment of the gaseous mixture (Fig. 2), TEG and CS_2, respectively, depleted by 6.7% (0.33 Torr) and 8.6% (0.86 Torr) and ethyne was formed in an amount corresponding to a depletion of TEG by ~1% (0.05 Torr). Independent 7 h irradiation of pure TEG did not produce any aerosol particles, but resulted in a depletion of TEG by only ~2.5% (0.12 Torr) and formation of ethyne in three times greater amount than in the presence of CS_2 (Fig. 3). These experiments showed that (1) in the gaseous mixture, CS_2 was consumed from the gas phase 2.5 times more efficiently than TEG, (2) TEG consumption was increased in the presence of CS_2, and (3) decomposition of TEG as revealed from the production of ethyne was suppressed in the gaseous mixture under conditions of CS_2 depletion (i.e. 0.05 Torr versus 0.12 Torr).

CS_2 molecule has an absorption band in the 270–350 nm region and absorbs the photon of the N_2 laser efficiently. It can be therefore envisaged that CS_2 is consumed from the gas phase through its polymerization [17–21,26–28]. On the other hand, TEG has the longest wavelength absorption band below 230 nm. Hence, its photolysis is due to two-photon absorption of N_2 laser light. TEG can, in fact, be decomposed via three possible routes that are homolysis of the Ge–C bond (Scheme 1), molecular expulsion of ethyne (Scheme 2), or molecular expulsion of buta-1,3-diene (Scheme 3).

$(H_2C{=}CH)_4Ge \rightarrow H_2C{=}CH\cdot + {}^{\cdot}Ge(CH{=}CH_2)_3$

$H_2C{=}CH\cdot + (H_2C{=}CH)_4Ge \rightarrow C_2H_4 + {}^{\cdot}C(H){=}CH\text{-}Ge(CH{=}CH_2)_3$

${}^{\cdot}C(H){=}CH\text{-}Ge(CH{=}CH_2)_3 \rightarrow C_2H_2 + {}^{\cdot}Ge(CH{=}CH_2)_3$

Scheme 1.

$(H_2C{=}CH)_4Ge \rightarrow HC{\equiv}CH + HGe(CH{=}CH_2)_3 \rightarrow\rightarrow\rightarrow 4\,HC{\equiv}CH + GeH_4$

$(GeH_4 \rightarrow Ge + 2\,H_2)$

Scheme 2.

$(H_2C{=}CH)_4Ge \rightarrow \mathbf{:}Ge(CH{=}CH_2)_2 + H_2C{=}CH\text{-}CH{=}CH_2$

Scheme 3.

The absence of ethene and buta-1,3-diene and the occurrence of only the traces of ethyne among the volatile products strongly suggest that the major operating channel of photolysis of pure TEG follows to Scheme 2. Considering

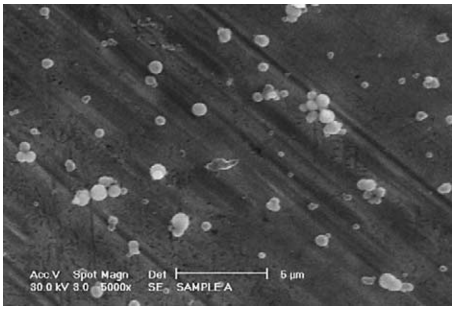

Fig. 4. SEM image of sedimentary particles deposited from a gaseous mixture of CS_2 (20 Torr) and TEG (5 Torr) under N_2 laser irradiation at an energy of 1.8 mJ/pulse for 4 h. Original magnification of SEM, 5000×.

the facts that in the gaseous mixture, decomposition of TEG was suppressed but TEG consumption was increased, the major operating channel of the photochemical reactions in the gaseous mixture is the incorporation of TEG molecule into the polymerizing CS_2. This is further supported from XPS result (discussed later) that the major chemical species of Ge is assignable to Ge bonded to carbon atoms.

3.2. *Properties of the aerosol particle*

SEM image of the aerosol particles deposited from a gaseous mixture of CS_2 (20 Torr) and TEG (5 Torr) under N_2 laser light irradiation (Fig. 4) revealed that the particles are spherical with a mean diameter of 0.4 μm.

The atomic abundance of these particles was determined from both EDX and XPS analyses. The atomic ratios are 56–59% C, 3–4% Ge, 28–30% S and 8–13% O by EDX; and 57–69% C, 0.5–1.2% Ge, 9–15% S and 15–28% O by XPS method. These analyses revealed the signal of the Cu substrate (coming from the uncovered surface), which indicates that some fraction of the O and also of the C signals can originate from the surface contamination and oxidation of the substrate present prior to particle deposition. Disregarding the oxygen values and considering that carbon values are somewhat lower, the EDX and XPS data are close to those (63.3% C, 6.0% Ge and 30.7% S) estimated from the measured depletion of CS_2 and TEG from the gas phase. This agreement shows that the elements depleted from the gas phase are efficiently utilized for the formation of the solid product and that they do not escape into the gas phase.

The XPS analysis was performed on the sedimentary aerosol particles deposited on a Cu sheet from a gaseous mixture of CS_2 (20 Torr) and TEG (5 Torr) and from pure CS_2 (50 Torr). The stoichiometry of atoms are $S_{1.00}$ $C_{4.50}$ $O_{0.97}$ $Ge_{0.08}$ ($Cu_{0.33}$), and $S_{1.00}$ $C_{3.00}$ $O_{1.11}$ ($Cu_{0.31}$), for the deposits from the gaseous mixture and from pure CS_2, respectively. The XPS spectra of the C 1s and S 2p photoelectrons are shown in Fig. 5. Considering the splitting due to spin-orbit coupling of S 2p band, the results are summarized in Table 1. The particles deposited from both CS_2 and the CS_2–TEG mixture contain sulfur atoms in a $(-C-S-)_n$ bonding (and partly in elemental sulfur) as a major contribution (see Fig. 5A). About 25% of sulfur can be assigned to sulfur in >C=S or Cu–S bonding, and remaining ∼3% to sulfidic and/or S–O– moiety [36–38]. These latter two contributions likely result from a reaction of S with Cu substrate and with atmospheric oxygen. In the C 1s spectrum of the aerosol particles, carbon belonging to the $(-C-S-)_n$ bonding was detected at 285.6 eV. The binding energies (284.5 and 288.1 eV) of components of the C 1s spectrum are compatible with carbon contained in C–C and C–H bonds (major components), and C–O and C=O bonds (minor components). The atomic ratio of S and C atoms pertinent to the C–S bonding was evaluated using the experimentally determined stoichiometry of atoms to be 0.73:0.81 and 0.72:0.81 for the particles deposited from the gaseous mixture and from pure CS_2, respectively. The values, which are very close to unity, clearly support that the major chemical species of polymeric particles is $(-C-S-)_n$ polymer as reported previously [39]. The binding energy of the Ge $2p_{3/2}$ electrons is best accounted for

Table 1
XPS characterization of aerosol particles deposited from pure CS_2 and a gaseous mixture of CS_2 and TEG

Irradiated sample	Line designation	Binding energy (eV)	Population (%)	Assignment [36–38]
CS_2 (50 Torr)	S $2p_{3/2}$	162.0	22	>C=S[a], Cu–S
		163.7	72	$(CS)_n$ polymer
		167.9	6	S–O
	C 1s	284.4	59	C–C, C–H
		285.5	27	$(CS)_n$ polymer
		287.1	7	C–O
		288.5	7	C=O
CS_2 (20 Torr) + TEG (5 Torr)	Ge $2p_{3/2}$	1218.7	100	C–Ge–C
	S $2p_{3/2}$	162.1	25	>C=S[a], Cu–S
		163.6	73	$(CS)_n$ polymer
		167.9	2	S–O
	C 1s	284.5	73	C–C, C–H
		285.6	18	$(CS)_n$ polymer
		288.1	9	C=O

[a] This assignment is based on our measurements of S $2p_{3/2}$ binding energies for 4,4′-bis(dimethylamino)thiobenzophenone and 10-methylacridine-9-thione used as standards.

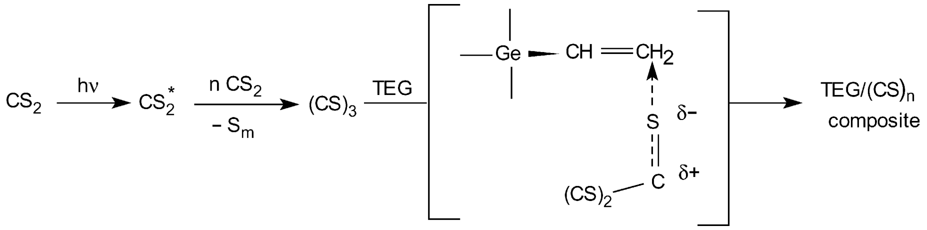

Scheme 4.

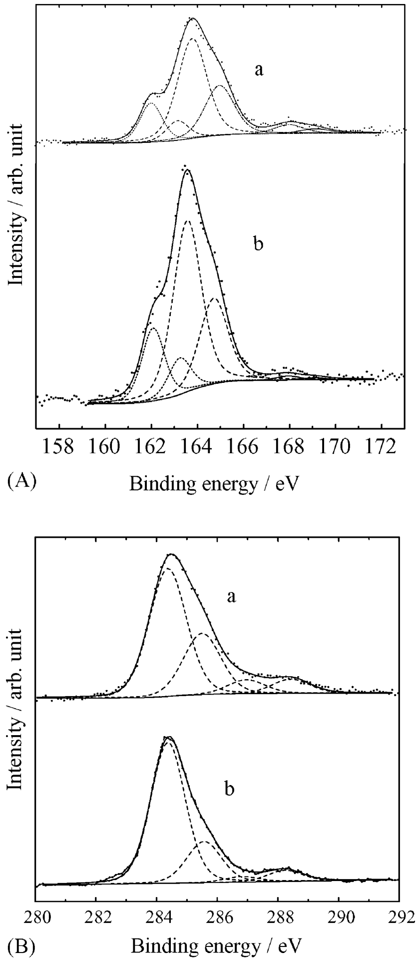

Fig. 5. Fitted spectra of (A) S 2p and (B) C 1s electrons of the sedimentary particles produced from (a) pure CS_2 (50 Torr) and (b) a gaseous mixture of CS_2 (20 Torr) and TEG (5 Torr).

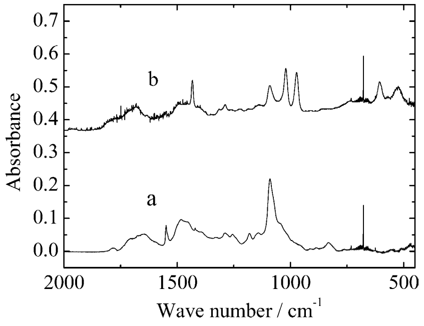

Fig. 6. FT-IR spectra of the sedimentary particles deposited from (a) pure CS_2 (50 Torr) and (b) a gaseous mixture of CS_2 (50 Torr) and TEG (5 Torr) under N_2 laser irradiation at an energy of 1.8 mJ/pulse for 3 h.

by Ge bonded to carbon atoms, supporting the incorporation of TEG molecules into polymerizing CS_2, i.e. into highly crosslinked $(–C–S–)_n$ polymer.

The aerosol particles produced from CS_2 under N_2 laser light irradiation show IR spectral pattern (Fig. 6a) having contributions of ν(C=C) [40] at 1600 and 1440 cm^{-1}, ν(C–C) at 1224 and 1257 cm^{-1}, ν(C=S) at 1066 cm^{-1} and ν(C–S) at 818 cm^{-1}, which is similar to that of the $(CS_2)_x$ polymer deposited from gaseous CS_2 by irradiation at 313 nm [27]. The FT-IR spectra of the aerosol particles deposited from the CS_2–TEG mixture (Fig. 6b) contain additional bands at 1391, 1000 and 953 cm^{-1} assignable to $\delta(GeCH{=}CH_2)$ [41] and bands at 605 and 528 cm^{-1} that are due to ν(Ge–C) vibration [42]. These spectra thus lend additional support for the incorporation of tetravinylgermane and reveal that significant fraction of ethenyl groups are preserved in the polymer.

The XPS and FT-IR spectral data and the depletion of both CS_2 and TEG from the gas phase are thus compatible with incorporation of TEG molecule in $(CS)_n$ species ($n = 2-3$) with C=S group through co-polymerization at the ethenyl bond. We presume that the addition proceeds by nucleophilic attack of the S atom at the β-carbon (Scheme 4), since this mechanism has some analogy in the known reactions of organogermanium compounds [42,43]

We compare here the reported process to the N_2 laser-induced formation of aerosol particles from the gaseous mixture of acrolein and CS_2 [23] or methyl acrylate and CS_2 [24,25], in which the produced sedimentary particles possessed features of poly(acrolein) and poly(methyl acrylate). Conversely to these well-polymerizing common monomers, olefinic derivatives of germanium hardly tend to polymerize in the absence of catalysts [43] and the N_2 laser-induced formation of aerosol particles from the gaseous mixture of TEG and CS_2 represents an exceptional and feasible process of co-polymerizing a single TEG molecule into the polymerizing CS_2. It is noteworthy that analysis of XPS strongly suggested the chemical structure of the sedimentary aerosol particles from CS_2 being highly crosslinked $(–C–S–)_n$ polymer when irradiated with N_2 laser light. This also reflects a variety of chemical reactivity of C=S bond.

Acknowledgements

This work was supported by the Japan Society for the Promotion of Science and by the Ministry of Education, Youth and Sports of the Czech Republic (grant No. ME612) and in part by Grant-in-Aid for Scientific Research on Priority Area “Innovative utilization of strong magnetic fields” (Area 767, No. 15085203) from MEXT of Japan.

References

[1] J. Pola, J. Anal. Appl. Pyrol. 30 (1994) 73.
[2] M. Urbanová, J. Vítek, Z. Bastl, K. Ubik, J. Pola, J. Mater. Chem. 5 (1995) 849.
[3] J. Pola, Rad. Phys. Chem. 49 (1997) 151.
[4] J. Pola, H. Morita, Tetrahedron Lett. 38 (1997) 7809.
[5] J. Pola, M. Urbanová, Z. Bastl, H. Morita, Macromol. Rapid Commun. 21 (2000) 178.
[6] J. Pola, M. Urbanová, Z. Bastl, J. Šubrt, M. Sakuragi, A. Ouchi, H. Morita, Polymer 42 (2001) 1311.
[7] J. Pola, J. Vítek, Z. Bastl, J. Šubrt, J. Organomet. Chem. 640 (2001) 170.
[8] J. Pola, A. Galíková, A. Galík, V. Blechta, Z. Bastl, J. Šubrt, A. Ouchi, Chem. Mater. 14 (2002) 144.
[9] M.A. El-Sayed, Acc. Chem. Res. 34 (2001) 257.
[10] H. Morita, J. Photopolym. Sci. Technol. 12 (1999) 95.
[11] J. Pola, Surf. Coat. Technol. 100–101 (1998) 408, and references therein.
[12] J. Pola, M. Urbanová, V. Dřínek, J. Šubrt, H. Beckers, J. Mater. Chem. 9 (1999) 2429.
[13] J. Pola, A. Lyčka, L.E. Gusel’nikov, V.V. Volkova, J. Chem. Soc. Chem. Commun. (1992) 20.
[14] H. Morita, T. Sadakiyo, J. Photochem. Photobiol. A 87 (1995) 163.
[15] H. Morita, K. Semba, T. Umezawa, M. Kuwamura, Colloids Surf. A 153 (1999) 203.
[16] H. Morita, M. Shimizu, J. Phys. Chem. 99 (1995) 7621.
[17] K. Ernst, J.J. Hoffman, Chem. Phys. Lett. 68 (1979) 40.
[18] K. Ernst, J.J. Hoffman, Phys. Lett. 87A (1981) 133.
[19] Y.P. Vlahoyannis, E. Patsilinakou, C. Fotakis, J.A.D. Stockdale, Radiat. Phys. Chem. 36 (1990) 523.
[20] A. Matsuzaki, H. Morita, Y. Hamada, Chem. Phys. Lett. 190 (1992) 331.
[21] A. Matsuzaki, Y. Hamada, H. Morita, T. Matsuzaki, Chem. Phys. Lett. 190 (1992) 337.
[22] R. Tomovska, Z. Bastl, V. Vorlíček, K. Vacek, J. Šubrt, Z. Plzák, J. Pola, J. Phys. Chem. B 107 (2003) 9793.
[23] H. Morita, Y. Kimura, M. Kuwamura, T. Watanabe, J. Photochem. Photobiol. A 103 (1997) 27.
[24] H. Morita, K. Kanazawa, J. Photochem. Photobiol. A 112 (1998) 81.
[25] H. Morita, H. Haga, J. Photopolym. Sci. Technol. 8 (1995) 475.
[26] F.C. Wen, T. McLaughlin, J.L. Katz, Phys. Rev. A 26 (1982) 2235.
[27] J.J. Colman, W.C. Trogler, J. Am. Chem. Soc. 117 (1995) 11270.
[28] A. Matsuzaki, J. Mol. Struct. (Theochem) 310 (1994) 95.
[29] F. Cataldo, Inorg. Chim. Acta 232 (1995) 27.
[30] J. Pola, R. Fajgar, Z. Bastl, L. Diaz, J. Mater. Chem. 2 (1992) 961.
[31] R. Fajgar, Z. Bastl, J. Tláskal, J. Pola, Appl. Organometal. Chem. 9 (1995) 667.
[32] E.G. Rochow, in: J.C. Bailar, H.J. Emeléus, R. Nyholm, A.F. Trotman-Dickenson (Eds.), Comprehensive Inorganic Chemistry, Vol. 2, Pergamon Press, Oxford, 1973, pp. 1–41.
[33] M. Jakoubková, Z. Bastl, P. Fiedler, J. Pola, Infrared Phys. Technol. 35 (1994) 633.
[34] K. Semba, H. Morita, J. Photochem. Photobiol. A 150 (2002) 7.
[35] D. Seyferth, J. Am. Chem. Soc. 79 (1957) 2738.
[36] G. Beamson, D. Briggs, High Resolution XPS of Organic Polymers: the Scienta ESCA 300 Database, Wiley, 1992.
[37] C. Wagner, J.A. Taylor, J. Electron Spectrosc. Relat. Phenom. 28 (1982) 211.
[38] D. Briggs, M.P. Seah (Eds.), Practical Surface Analysis. Auger and X-ray Photoelectron Spectroscopy, Vol. 1, Wiley, Chichester, 1990, p. 595.
[39] H. Sontag, A.C. Tam, P. Hess, J. Chem. Phys. 86 (1987) 3950.
[40] P.B. Zmolek, H. Sohn, P.K. Gantzel, W.C. Trogler, J. Am. Chem. Soc. 123 (2001) 1199.
[41] M. Lesbre, P. Mazerolles, J. Satge, The Organic Compounds of Germanium, Wiley, London, 1971.
[42] J. Cross, F. Glockling, J. Organomet. Chem. 3 (1965) 146.
[43] P. Riviere, M. Riviere-Baudet, J. Satge, in: G. Wilkinson, F.G.A. Stone, E.A. Abel (Eds.), Comprehensive Organometallic Chemistry, Pergamon Press, Oxford, 1982.